



Assessing the potential for DMS enrichment at the sea-surface and its influence on air–sea flux

C.F. Walker¹, M.J. Harvey¹, M.J. Smith¹, T.G. Bell^{2,3}, E.S. Saltzman³, A.S. Marriner¹, J.A. McGregor¹, C.S. Law^{1,4}

5 ¹ National Institute of Water and Atmospheric Research, Wellington, New Zealand

² Plymouth Marine Laboratory, Plymouth, United Kingdom

³ University of California, Irvine, United States of America

⁴ Department of Chemistry, University of Otago, Dunedin, New Zealand

Correspondence to: C.F. Walker (carolyn.walker@royalsociety.org.nz)

10 Alternative email: C.S. Law (cliff.law@niwa.co.nz)

Abstract. The flux of dimethylsulfide (DMS) to the atmosphere is generally inferred using water sampled at or below 2 m depth, thereby excluding any concentration anomalies at the air–sea interface. Two independent techniques were used to assess the potential for near-surface DMS enrichment to influence DMS emissions and also identify the factors influencing enrichment. DMS measurements in productive frontal waters over the Chatham Rise, east of New Zealand, did not identify
15 any significant DMS gradients between 0.01 and 6 m in sub-surface seawater, whereas DMS enrichment in the sea-surface microlayer was variable, with a mean enrichment factor (EF; the concentration ratio between DMS in the SSM and in sub-surface water) of 1.7. Physical and biological factors influenced sea-surface microlayer DMS concentration, with high enrichment (EF > 1.3) only recorded in a dinoflagellate-dominated bloom, and associated with low to medium wind speeds and near-surface temperature gradients. On occasion, high DMS enrichment preceded periods when the air–sea DMS flux,
20 measured by eddy covariance, exceeded the flux calculated using COARE parameterised gas transfer velocities and measured sub-surface seawater DMS concentrations. The results of these two independent approaches suggest that air–sea emissions may be influenced by near-surface DMS production under certain conditions, and highlights the need for further study to constrain the magnitude and mechanisms of DMS production in the sea surface microlayer.

1 Introduction

25 In remote, relatively pristine marine environments such as the Southern Ocean, the production of aerosols and clouds is predominantly governed by natural sources. In order to represent these sources in Earth system models and project their response to climate change, the exchange of volatiles between the atmosphere and ocean requires rigorous constraint. Dimethylsulfide (DMS) is derived from phytoplankton, and constitutes the largest natural source of non-sea-salt sulfate aerosol to the global troposphere of 10–20 nmol L⁻¹ h⁻¹ (Simó, 2001; Andreae and Crutzen, 1997), with an estimated annual



input of 28.1 Tg S (Lana et al., 2011). Once in the atmosphere, DMS reacts to form sulfate aerosol, which acts as a source of cloud condensation nuclei. DMS-derived aerosols may thus have a significant impact on the radiation budget, via direct scattering of sunlight and changes to cloud properties (Charlson et al., 1987;Andreae and Crutzen, 1997;Ayers and Gillett, 2000). However, current global flux estimates of DMS are poorly constrained, with estimates varying by as much as a factor of two (Lana et al., 2011).

Direct measurements of the air–sea exchange or flux (F) of a gas are challenging and so F is often computed using an empirically determined gas transfer coefficient (k) and the air–sea concentration disequilibria (ΔC), according to the equation $F = k\Delta C$ (Liss, 1983). The variability in flux estimates is widely considered to be driven by uncertainties in k (Zemmelink et al., 2004), which have been determined by a variety of methods including field observations using deliberately released tracers (Nightingale et al., 2000;Wanninkhof et al., 2004;Ho et al., 2011), wind and wave tank experiments (McGillis et al., 2000), global oceanic ^{14}C uptake (Sweeney et al., 2007), and simultaneous measurements of water-side gas concentrations and air–sea flux (Huebert et al., 2004;Marandino et al., 2009;Bell et al., 2013). As gas exchange is primarily driven by shear-generated turbulence, k is often parameterised as a function of wind speed (Liss and Merlivat, 1986;Wanninkhof, 1992;Ho et al., 2006). However, gas fluxes are inadequately modelled by wind speed alone (Blomquist et al., 2006;Zemmelink et al., 2004), as other factors such as wave-breaking, sea-state (e.g. Woolf, 2005;Asher et al., 1996), rain (e.g. Ho et al., 2000), and surface films (e.g. Schmidt and Schneider, 2011) also influence gas exchange at the sea-surface. To enable prediction of gas fluxes for a range of compounds including DMS, the National Oceanographic and Atmospheric Administration (NOAA) COARE model has been developed to incorporate many of the above factors. The model has been tuned to (Fairall et al., 2011) and validated against DMS eddy covariance field data (Blomquist et al., 2006;Yang et al., 2011).

The air–sea concentration disequilibria of DMS, and consequently air–sea exchange, are essentially controlled by the concentration in seawater ([DMS]) as atmospheric concentrations are typically at least two orders of magnitude lower. However, [DMS] is invariably measured at or below 2 m depth in both discrete and underway modes, and not at the sea-surface microlayer (SSM), the interface where gas exchange occurs. This assumes that there are no significant sources or sinks of DMS between the sample depth and the sea-surface. [DMS] in the surface mixed layer is generally determined by the biomass, activity and species composition of phytoplankton that produce dimethylsulfoniopropionate (DMSP), the precursor to DMS (Turner et al., 1988). Intracellular DMSP is regulated by factors such as nutrient availability and ultraviolet radiation dose (Archer et al., 2010;Toole and Siegel, 2004), whereas extracellular DMSP is influenced by grazing and bacterial processing (Yoch, 2002). To date, studies characterising near-surface [DMS] have shown a decreasing gradient towards the interface, indicative of degassing (Zemmelink et al., 2005). However, direct measurements of the air–sea flux of DMS by eddy covariance (EC) over coccolithophore-rich North Atlantic waters significantly exceeded those calculated from bulk seawater concentrations (Marandino et al., 2008). This discrepancy between predicted and observed fluxes was attributed to near-surface [DMS] gradients (above latitudes of 55 °N; Marandino et al., 2008).



Despite the biophysical challenge of maintaining a DMS source in a relatively thin (10–100 μm) layer at the air–water interface, a number of studies have examined and identified enrichment of DMS in the sea surface microlayer, as summarised in Fig. 1 and references therein. Microlayer thickness, as defined by near-surface biogeochemical gradients, is of the order of 100 μm (Zhang et al., 2003). Given the challenges of sampling this thin surface layer, the thickness has been operationally defined as 1 mm by Liss and Duce (1997). In the current paper we evaluate properties for both 100 μm and 1 mm thickness. The physico-chemical and biological properties of the SSM are often distinct from underlying waters, and may support enhanced biogeochemical activity (Liss and Duce, 1997). For example, the SSM is often enriched with surface-active organic material and bacteria, and is subject to elevated ultraviolet radiation and temperature (Cunliffe et al., 2013). DMS measurements in the SSM have identified both enrichment and depletion relative to sub-surface seawater (SSS) concentrations; however enrichment has tended to dominate (Fig. 1). The source and controls of this excess DMS have not been identified, and the assumption that the SSM may influence DMS emissions to the atmosphere remains untested.

A variety of devices have been successfully deployed for sampling biological assemblages and dissolved compounds in the SSM (Cunliffe and Wurl, 2014). Trace gas SSM analyses are more challenging given the difficulties of sampling a volatile gas in a thin film that is subject to air- and water-side turbulence. Indeed, laboratory experiments have shown that a proportion of DMS is inevitably lost during SSM sampling, regardless of the device used (Yang et al., 2001). The aim of this work was to test the potential for near-surface processes to influence air–sea DMS exchange using a novel combination of direct sampling of the SSM and SSS, and EC measurement of air–sea DMS flux. Measurements were made during the Surface Ocean Aerosol Production (SOAP) voyage (Bell et al., 2015; Law C. S. et al., submitted). The influence of biogeochemical variability on spatial and temporal variation in near-surface DMS enrichment and flux was assessed by measurements in three phytoplankton blooms of differing community composition in productive frontal waters east of New Zealand. This location is currently under-represented in the global DMS database and climatology (Kettle and Andreae, 2000; Lana et al., 2011). In addition, the meteorological and physical factors influencing near-surface [DMS] were also examined in this assessment of DMS enrichment in the SSM and its potential contribution to air–sea flux.

2 Methodology

2.1 Study location

Sampling was conducted aboard the R/V *Tangaroa* between February and March 2012 along the Chatham Rise, an underwater plateau separating sub Antarctic and subtropical waters in the South-West Pacific, east of New Zealand. This is a region of high productivity in which frontal activity enhances mixing in the water column, fostering large phytoplankton blooms in the spring and summer seasons (Murphy et al., 2001). Satellite imagery in combination with continuous measurement of surface (6 m depth) chlorophyll-*a* fluorescence and seawater DMS, measured by atmospheric pressure chemical ionization mass spectrometry (API-CIMS; Bell et al., 2015), were used to locate phytoplankton blooms for



focussed studies on a range of air–sea parameters during the SOAP voyage (Law C. S. et al., submitted). SSM and SSS sampling were undertaken in three distinct blooms: B1 (DOY 45.8 to 48.8), B2 (DOY 52.8 to 55.0), and B3 (DOY 58.1 to 65.1), located as shown in Fig. 2. Day of year (DOY) is defined as 1 on January 1st at 00:00 h

2.2 Seawater collection

5 Near-surface seawater samples were collected from a rigid-hulled inflatable boat (RHIB) during periods of low swell and wind speeds $<10 \text{ m s}^{-1}$. The light wind conditions reduced both DMS loss during collection (Zemmelink et al., 2005) and physical disruption of the *in situ* SSM (Carlson, 1983). The RHIB was positioned at least 500 m upwind of the R/V *Tangaroa* to avoid ship-borne contamination and artefacts associated with downstream turbulence. A total of 11 SSM stations were sampled, with station coordinates and sampling dates and times indicated in Table 1.

10 2.2.1 Sea-surface microlayer

A number of devices have been used to sample the SSM, but there have been few comparisons of techniques (Cunliffe and Wurl, 2014 and references therein). In this study the Harvey glass plate (Harvey, 1966; Harvey and Burzell, 1972) and Garrett metal screen (Garrett, 1965) were deployed as these are two of the most frequently used techniques (see Fig. 1). The glass plate works on the principle that the microlayer adheres to its surface as it is withdrawn, while the screen relies on surface tension to trap SSM water and matter in the interstitial spaces within a wire grid. The surface areas of the rectangular plate and round screen (with 0.6 mm wires) were 600 and 804 cm^2 , respectively. The glass plate was silanised to avoid DMS loss through surface adsorption. Samplers were inserted vertically into the sea-surface on the downwind side of the boat where the SSM was less disturbed. The plate was slowly removed in the vertical position, whereas the screen was rotated 90° while submerged and then removed at a near-horizontal angle. Seawater adhering to the collection device was immediately drained through a funnel into prewashed 30 ml glass serum bottles for 30 seconds. Although a wiper is often used with the plate for sampling particulates and surfactants (Cunliffe and Wurl, 2014), this was not used in the current study to avoid DMS loss and potential disruption of algal cells. DMS concentrations in the SSM are referred to herein as $[\text{DMS}_{\text{SSM}}]$.

2.2.2 Sub-surface water

In addition to the SSM, seawater for the determination of $[\text{DMS}]$ was collected in duplicate from four sub-surface depths (<1 , 7, 30, and 162 cm) in 150 ml crimp top, glass bottles that were pre-washed in a solution of phosphate-free detergent and rinsed with ultrapure water. Seawater from just below the SSM was collected using a “sipper”, with seawater pumped from a network of floating silicone tubes (each ~300 mm long and 3.2 mm outer diameter) using a peristaltic pump into a collection bottle. The tube intake ends were slightly weighted, to minimise disturbance of the SSM and air bubble introduction, for sampling at a depth of 1–2 cm that precluded the SSM. Seawater from depths of 7, 30, and 162 cm was collected using three fixed-depth stainless steel tubes attached to a floating buoy and connected to a peristaltic pump. Samples from 162 cm



(referred to herein as $[DMS_{1.6m}]$) were assessed for pump-associated artefacts by comparison with samples collected at 2 m depth using standard Niskin bottles on a CTD rosette. The latter was collected within one hour of the RHIB sampling. A Wilcoxon signed-ranks test for paired samples with non-parametric distributions indicated no significant ($p = 1$, $\alpha = 0.5$) difference between the two approaches.

5 2.3 Analytical methods

2.3.1 Seawater DMS (continuous)

$[DMS]$ was continuously measured in the ships seawater intake (6.0 m depth; $[DMS_{6.0m}]$) using an atmospheric pressure chemical ionization mass spectrometer equipped with a porous membrane equilibrator, UCI Mini-CIMS (Bell et al. (2013)). A one hour moving average algorithm was used to smooth $[DMS_{6.0m}]$.

10 2.3.2 Seawater DMS (discrete)

Discrete seawater samples were analysed for DMS while at sea using a semi-automated purge and trap system with a HP 6850 gas chromatograph interfaced with an Agilent flame photometric detector (Walker et al., 2000) up until DOY 47.0. An Agilent (Sievers) 355 sulphur chemiluminescent detector (SCD) was used after DOY 47.0. Seawater samples were gently filtered through an inline 25 mm GF/F filter to remove particulates, and a calibrated volume (5 ml) of the filtrate transferred to a 10 ml silanised glass chamber fitted with a quartz frit and purged with zero-grade nitrogen (99.9% pure). The chamber and frit were cleaned daily with 5% HCl and ultrapure water to prevent organic matter build-up. The GF/F filter was changed between each sample and the filter holder rinsed with ultrapure water. Gas phase DMS was cryogenically concentrated on 60/80 Tenax TA in a 1/8" Restek Sulfinert-treated stainless steel trap at -20°C and thermally desorbed at 100°C for GC analysis.

20 Calibration was carried out using two temperature controlled VICI Metronics wafer permeation tubes, one filled with methylethylsulphide (MES) and the other DMS. MES was used as an internal standard, with samples doped during analysis to allow for correction of short-term changes in detector sensitivity. The DMS permeation tube, housed in a dynacalibrator, provided the external standard. A five-point calibration was performed twice per day, and a running standard every 12 samples. A subsequent international intercalibration (Swan et al., 2014) indicated that the analytical method was $93.5 \pm 3.8\%$ accurate with 2.6% variation. Blank samples were tested regularly, using both ultrapure water and DMS-free seawater from a depth of 500 m, with a mean blank of $< 0.1 \text{ nmol L}^{-1} [DMS]$.

Water samples were analysed within 5 hours of collection. Throughout the voyage, the SCD and Mini-CIMS techniques were compared using seawater from the ship's intake system. The SCD technique gave slightly higher concentrations, with the mean of the residuals indicating an average difference of $1.2 \text{ nmol L}^{-1} \text{ DMS}$ (Fig. 3). This difference is possibly attributable to DMS production during sample storage prior to SCD analysis, as deck incubation of SSS and SSM water from B2 and B3 indicated mean in-bottle production rates in the dark of $0.23 \text{ nmol L}^{-1} \text{ h}^{-1}$ (Cliff Law, pers. comm.); a total



production of 1.2 nmol L^{-1} over 5 hours. In addition, the deviation from the 1:1 line of [DMS] in samples with both low and high storage times, suggests storage time is not a significant driver of the difference between the two analytical techniques (Fig. 3). Further investigation also showed a lack of relationship between analysis time and EF, particularly for B1 samples ($r^2 = 0.002$) suggesting that there was no significant DMS production between collection and analysis.

5 2.3.3 SSM enrichment factors

The anomaly between the SSM and underlying SSS is indicated by the enrichment factor (EF), the concentration ratio between DMS in the SSM and at 1.6 m depth:

$$EF = ([\text{DMS}]_{\text{ssm}}) / ([\text{DMS}]_{1.6\text{m}}) \quad (1)$$

EFs were calculated using [DMS_{1.6m}] from the RHIB, rather than [DMS_{6.0m}] from the ship's CTD, to minimise error arising from spatio-temporal variability. An $EF > 1$ indicates DMS enrichment and < 1 indicates DMS depletion, in the SSM.

2.3.4 Eddy covariance-derived DMS air–sea flux

Although the basic principles of turbulent flux exchange are well-established (Swinbank, 1951), refinements have been made to adapt the micrometeorological technique of EC for use on a moving platform (e.g. Edson et al., 1998). In addition, the development of atmospheric pressure chemical ionization mass spectrometry (API-CIMS) for high frequency DMS measurement (Bandy et al., 2002; Huebert et al., 2004; Marandino et al., 2007) has enabled direct measurements of air–sea DMS flux on time-scales on the order of tens of minutes. By combining water- and air-side gas concentrations, these high-resolution measurements allow the response of k in relation to spatial variation in biological and environmental conditions to be determined. In the current study, continuous measurement of air–sea DMS flux at 10 minute intervals on the ship's bow was achieved using EC and API-CIMS, as described in Bell et al. (2013). EC flux data (F_{EC}) were smoothed using a moving average algorithm with a span of 1 hour, and used to calculate the inferred DMS concentration in surface waters (see Sect. 2.4.2).

2.3.5 Near-surface temperature gradients

A spar buoy was deployed in each bloom for autonomous sampling of near-surface temperature gradients. Temperature loggers (RBR TR-1060) recorded temperature at 0.5 m intervals between 0.25 and 4.25 m depth, with deployments typically lasting 4 days.

2.4 Computations

2.4.1 Air–sea DMS fluxes

DMS flux (F_{DMS}) was calculated using the gas transfer coefficient k and the concentration difference at the air–sea interface according to:



$$F_{\text{DMS}} = k(C_w - \frac{C_a}{H}) \quad (2)$$

where H is the dimensionless Henry's law solubility coefficient for DMS (Dacey et al., 1984), C_w is $[\text{DMS}_{6.0\text{m}}]$, and C_a is the DMS concentration measured in air. Most conceptual models assume that k is dependent on molecular diffusion across the surface layer, the thickness of which is modulated by near-surface turbulent processes (Liss and Slater, 1974). For DMS in temperate waters, the waterside diffusive layer provides the dominant control on air–sea flux. This assumes there is no significant internal loss or production in the thin diffusive layer at the surface (Nightingale, 2013), and also that there is more rapid mixing below. The transfer velocity k was calculated using the NOAA COARE model (version 3.1g; Fairall et al., 2011), and parameterised in terms of local wind speed scaled to 10 m height, as in Bell et al (2015). k was then adapted for DMS using the Schmidt number for local seawater temperature and salinity at 6.0 m depth (Saltzman et al., 1993).

2.4.2 Flux-inferred seawater [DMS]

The inferred DMS concentration in surface waters ($[\text{DMS}_{\text{inf}}]$) required to support the observed air–sea flux was derived from Eq. (2), using the measured EC flux, F_{EC} , and a k predicted by the NOAA COARE model, which incorporates bulk meteorological variables including wind speed, temperature and stability (Bell et al., 2015). To generate $[\text{DMS}_{\text{inf}}]$ at the same sampling frequency as the smoothed $[\text{DMS}_{6.0\text{m}}]$, k was calculated at ten minute intervals and smoothed using a moving average algorithm with a span of 1 hour. To facilitate comparison with $[\text{DMS}_{\text{SSM}}]$, a mean $[\text{DMS}_{\text{inf}}]$ was generated for each RHIB station for the period three hours before SSM sampling until five hours afterwards.

2.4.3 DMS production in the SSM

The excess or residual [DMS] in the SSM, relative to underlying waters, was calculated using two independent approaches. Subtracting $[\text{DMS}_{1.6\text{m}}]$ from $[\text{DMS}_{\text{SSM}}]$ provided an estimate of *SSM-derived residual [DMS]*, the excess [DMS] in the SSM determined by direct measurement. A second approach was to subtract the observed $[\text{DMS}_{6.0\text{m}}]$ from the estimated $[\text{DMS}_{\text{inf}}]$ to derive an estimate of *EC-derived residual [DMS]*, the excess [DMS] in the SSM calculated indirectly from flux measurements. The latter was used to estimate the net DMS production rate in the SSM (PR_{SSM}) required to support the observed air–sea flux:

$$\text{PR}_{\text{SSM}} = \frac{F_{\text{EC}} - F_{6.0\text{m}}}{z} \quad (3)$$

where F_{EC} is the flux measured by EC, $F_{6.0\text{m}}$ is the flux estimated using $[\text{DMS}_{6.0\text{m}}]$ and Eq. (2), and z is the SSM thickness (100 μm and 1 mm). As PR_{SSM} was calculated using the measured and expected DMS flux, it is independent of the measured $[\text{DMS}_{\text{SSM}}]$.



3 Results

3.1 Comparison of SSM sampling techniques

Comparison of $[DMS_{SSM}]$ measured by the Garret metal screen and Harvey glass plate, using Wilcoxon signed-ranks test for paired samples, indicated a significant difference in results ($p = 0.0078$, $\alpha = 0.05$), with mean $[DMS_{SSM}]$ from plate sampling 42% lower than the Garret screen. This difference was substantially greater than the sampling blanks, which were determined using both ultrapure water and seawater from 500 m depth (consistently $< 0.3 \text{ nmol L}^{-1}$ DMS for both devices; 1.6% of the average sample concentration). One potential factor is that the Garret screen collects thicker SSM samples than the plate (Cunliffe and Wurl, 2014); however, there are also other differences in collection efficiency between the two methods. The screen is considered to recover more of the phytoplankton assemblage than the plate (Momzikoff et al., 2004; Agogu   et al., 2004). In the current study, the screen appeared to trap aggregates, particularly in B1, and this may have led to overestimates of $[DMS_{SSM}]$. Consequently, we will only discuss SSM data collected using the plate method, as these provide more conservative estimates of DMS enrichment in the SSM.

3.2 $[DMS]$ in the SSM and SSS

$[DMS_{SSM}]$ and $[DMS_{1.6m}]$ ranged from 3.8 to 41.5 nmol L^{-1} , and 4.9 to 13.8 nmol L^{-1} , respectively (Table 1, Fig. 4) and showed similar spatial variability to $[DMS_{6.0m}]$ (Fig. 5b, Bell et al., 2015). Maximum concentrations were observed in B1 (DOY 45.8 to DOY 48.8), with mean $[DMS_{SSM}]$ and $[DMS_{1.6m}]$ of $23.5 \pm 13.5 \text{ nmol L}^{-1}$ and $9.5 \pm 4.2 \text{ nmol L}^{-1}$, respectively, coincident with a mean $[DMS_{6m}]$ of $10.6 \pm 5.2 \text{ nmol L}^{-1}$ (range 2.9 - 24.7 nmol L^{-1}). B1 was dominated by dinoflagellates (Law C. S. et al., submitted), with a mean chlorophyll-*a* of 1.6 mg m^{-3} at 1–2 cm depth. A striking feature of B1 was the high $[DMS_{SSM}]$, which exceeded $[DMS_{6m}]$ (Fig. 5b), resulting in high average EFs (2.8 ± 2.0 , Table 1). Furthermore, two B1 stations exhibited EFs > 4.0 , which exceed the majority of $[DMS_{SSM}]$ maxima reported in the literature (Fig. 1). Conversely, B2 and B3 were characterised by lower $[DMS_{SSM}]$, which was typically indistinct from $[DMS_{6.0m}]$ (see Fig. 4). The mean $[DMS_{SSM}]$ and $[DMS_{SSS}]$ in B2 were 7.9 ± 1.2 and $7.0 \pm 0.1 \text{ nmol L}^{-1}$ respectively, with near-surface seawater at 1–2 cm depth of 1.0 mg m^{-3} chlorophyll-*a*, ~40% lower than B1, and dominated by coccolithophores. Although B3 was in a similar location to B1, it was temporally distinct with lower phytoplankton biomass (Law C. S. et al., submitted). Near-surface seawater was dominated by dinoflagellates and coccolithophores, with mean chlorophyll-*a*, $[DMS_{SSM}]$ and $[DMS_{1.6m}]$, of 0.8 mg m^{-3} , $6.5 \pm 2.8 \text{ nmol L}^{-1}$ and $8.0 \pm 2.0 \text{ nmol L}^{-1}$ respectively, and EFs near or below 1.0. Throughout the study there was no evidence of near-surface $[DMS]$ gradients between 1 cm and 1.6 m depth, including at the B1 stations exhibiting high levels of SSM enrichment (Fig. 4). The absence of near-surface DMS gradients was further confirmed by the agreement between $[DMS_{1.6m}]$ and $[DMS_{6.0m}]$ (Fig. 5b).



3.3 Inferred SSM [DMS]

F_{EC} was elevated during B1, with fluxes up to $\sim 100 \mu\text{mol m}^{-2} \text{d}^{-1}$ (Bell et al., 2015). Highest DMS fluxes were recorded between DOY 48.0 and 50.0 during B1, reflecting the elevated [DMS_{6.0m}] (Fig. 5b, Bell et al., 2015). [DMS_{inf}], the inferred DMS concentration in SSS required to support the EC flux, was calculated using NOAA COARE gas transfer coefficients and compared to [DMS_{6.0m}] (Fig. 5b). [DMS_{6.0m}] was used to represent SSS, since continuous measurement at this depth provided greater temporal resolution (Bell et al., 2015). Overall, comparison of [DMS_{inf}] and [DMS_{6.0m}] in Fig. 5b shows good agreement. Where [DMS_{inf}] and [DMS_{6.0m}] agree in magnitude (*e.g.* DOY 55.0 to 58.0) the application of [DMS_{6.0m}] and k provides a robust estimate of air–sea DMS flux. However, between DOY 44.8 and 52.0, and to a lesser extent between DOY 58.0 and 61.0, a disparity was apparent with anomalously high [DMS_{inf}] observed that were not reflected in [DMS_{6.0m}].

During these periods the use of [DMS_{6.0m}] with k would underestimate the DMS flux. This disparity is evident during B1 in the comparison of EC-derived and SSM-derived residual [DMS], with the maxima of these independent approaches appearing close to each other (Fig. 5c). EC- and SSM-derived residual [DMS] were significant during B1 occupation, with maximum values of 20 and 33 nmol L⁻¹, respectively, during Station 4 (DOY 47.7 to 48.1), whereas EC- and SSM-derived residual [DMS] were generally not significant in B2 and B3.

These trends are confirmed by comparison of [DMS_{6.0m}] and [DMS_{inf}] for each bloom period in Fig. 6a–c. B1 shows a positive anomaly in [DMS_{inf}] relative to [DMS_{6.0m}], particularly at elevated [DMS_{6.0m}], indicative of an additional source of DMS contributing to the flux. At two of the four stations during B1 the mean [DMS_{inf}] was significantly greater than the mean [DMS_{6.0m}], with this positive bias in [DMS_{inf}] in B1 generally highest at intermediate wind speeds (Fig. 6a). Conversely, B2 and B3 generally showed good agreement between [DMS_{inf}] and [DMS_{6.0m}], although there was evidence of a negative anomaly at low to intermediate wind speeds (Fig. 6b–c), and a positive anomaly at high wind speeds in B3 (Fig. 6c). Comparison of the mean EC- and SSM-derived residual [DMS] for each station confirmed that the B2 and B3 stations generally cluster around the zero intercept (Fig. 6d), as expected if near-surface DMS sources were negligible. Conversely, B1 stations exhibited significant deviation from the zero intercept, with two stations characterised by high EC- and SSM-derived residual [DMS] coincident with high EF. At both of these stations the SSM-derived residual [DMS] exceeded the EC-residual [DMS], which may reflect the spatial variability of DMS in the SSM, non-representativeness of the single-point SSM measurements, or methodological artefacts.

3.4. Meteorological influences on near–surface structure

B1 was sampled during a high pressure system with low wind speeds (mean $6.0 \pm 2.7 \text{ m s}^{-1}$; Fig. 5a and 7b) and calm sea-state (waves $< 0.2 \text{ m}$), conditions conducive to SSM formation and preservation. A brief atmospheric front traversed the region during B2 with winds reaching 18 m s^{-1} , and multiple weather fronts occurred during B3 including a period of sustained high wind speeds up to 30 m s^{-1} (Fig. 5a). At wind speeds $> 10 \text{ m s}^{-1}$ the SSM is disrupted, with its constituents dispersed and diluted by sub-surface water (Wurl et al., 2011), and ventilation increases. The influence of physical processes



on a potential SSM source of DMS was examined between DOY 45.5 and 49.5 in B1 by comparison of EC- and SSM-derived residual [DMS] with U_{10} (wind speed at a reference height of 10 m above the ocean) and near-surface temperature gradient (Fig. 7a–c). Low wind speeds reduce air–sea exchange and enhance near-surface stratification, providing optimal conditions for maintenance of the SSM and retention of DMS. If this is the case then the contribution of the SSM to DMS flux would be most significant when the SSM is subsequently ventilated upon an increase in wind speed. This scenario is apparent on DOY 47.0 to 48.0 when a period of low wind speeds ($< 3 \text{ m s}^{-1}$), significant near-surface temperature gradients ($\sim 1^\circ\text{C m}^{-1}$), and elevated SSM-derived residual [DMS] was followed by a period of higher wind speed ($\sim 5\text{--}8 \text{ m s}^{-1}$), during which the EC-derived residual [DMS] increased (Fig. 7). However, the high SSM-derived residual [DMS] was also recorded at wind speeds of 6–9 m/s during DOY 45.8, indicating that DMS enrichment in the SSM may be maintained at moderate wind speeds.

3.5 DMS production rates in the SSM

The SSM production rate, PR_{SSM} , was estimated by subtracting the expected flux, calculated using $[DMS_{6.0m}]$ and the COARE algorithm, from the observed air–sea flux, and dividing by the thickness of the SSM (Eq. 3). This approach assumes that DMS production in the SSM was the source of the ‘excess’ air–sea flux in B1, and also that other DMS loss terms (photolysis, bacterial oxidation and vertical diffusion to sub-surface water) were negligible. Mean PR_{SSM} was estimated using SSM thicknesses of 100 and 1000 μm . Assuming a thickness of 1000 μm , PR_{SSM} was 217 ± 162 , -80 ± 33 and 74 ± 22 for stations B1, B2 and B3 respectively (Table 1). An alternative microlayer thickness of 100 μm resulted in PR_{SSM} one order of magnitude higher. The large uncertainty for each estimate is partially attributable to variation in the measured F_{EC} and $[DMS_{6.0m}]$ (see Fig. 5b). This approach of estimating PR_{SSM} from flux measurements has several advantages in that it is independent of the measured $[DMS_{SSM}]$, integrates horizontal variability, eliminates inherent uncertainty in the wind speed–gas transfer relationship, and does not rely on a single-point SSM measurement.

4 Discussion

The results of two independent techniques to assess the potential contribution of the sea surface microlayer to the air–sea exchange of DMS provide intriguing evidence that this may be significant under certain physical and biological conditions. This study adds to a number of other reports of DMS enrichment in the SSM (Fig. 1), but raises challenging questions regarding the source and maintenance of elevated DMS in the SSM. Consequently it is instructive to consider the validity of these results, and the physical and biological factors that may influence DMS in the SSM.

Near-surface gradients in dissolved gases have been reported previously for DMS and carbon dioxide (Zemmelink et al., 2005; Calleja et al., 2005), with potential implications for air–sea flux estimates. The vertical DMS profile in near-surface waters in B2 and B3 was uniform (see Fig. 4) indicating that DMS production and loss terms, such as ventilation, bacterial



oxidation and photolysis, were in balance (Galí et al., 2013). Furthermore the profiles do not show significant near-surface depletion in [DMS], which has been previously reported and attributed to ventilation and photolysis (Kieber et al., 1996). The presence of significant DMS enrichment in the SSM at the B1 stations (Table 1) is surprising, as vertical diffusion from the SSM would be expected to elevate [DMS] immediately below the SSM. As elevated [DMS] was not apparent at 1–2 cm (Fig. 4), this suggests that density stratification and/or preferential retention of DMS in the SSM suppressed vertical diffusive losses from the SSM. Elevated [DMS_{SSM}] has been previously reported relative to concentrations at 25 cm depth, associated with near-surface density gradients arising from ice melt in the Weddell Sea (Zemmelink et al., 2005). The near-surface temperature data in the current study indicated episodic formation of a gradient in the upper 4 m at the B1 stations (see Fig. 7) and, assuming this gradient extended to the sea-surface, the resulting stratification may have created optimal conditions for SSM enrichment, with concentration and retention of phytoplankton whilst suppressing diffusive loss to sub-surface water. Furthermore, the presence of surfactants may have suppressed ventilation across the air–sea interface (Salter et al., 2011) under these conditions, leading to accumulation of DMS in the SSM.

The surface microlayer sampling, storage and analysis may have introduced potential artefacts, particularly for trace gases. The mesh screen sampling produced higher [DMS_{SSM}] than the plate, potentially due to preferential retention of algal and suspended material on the mesh as previously reported (Turner and Liss, 1985). These authors also reported significant DMS enrichment coincident with elevated sub-surface productivity, and partially attributed the enrichment to “stressing of microlayer organisms as a result of the sampling procedure”. This may have occurred in the current study in B1, as dinoflagellates are sensitive to shear stress (Wolfe et al., 2002), but this was not tested. However, in contrast to other applications (Cunliffe and Wurl, 2014), we avoided scraping the SSM off the glass plate to reduce transfer of particulate material and ventilation of DMS, and this may also have reduced shear stress and exposure time of the phytoplankton. Exposure to air during SSM sampling enhances DMS evasion, with ~ 50% loss at zero wind speed (Zemmelink et al., 2005), which suggests that the majority of previous SSM [DMS] measurements (see Fig. 1) are underestimates (Zemmelink et al., 2006).

This raises the question as to how DMS enrichment is maintained in the SSM whilst ventilation is occurring across the air–sea interface. Zemmelink et al. (2006) calculated a DMS residence time in the SSM on the order of 40–60 seconds, and consequently a very high production rate would be required to maintain enrichment. The PR_{SSM} estimates in Table 1, which are determined indirectly from F_{EC} and are independent of the SSM concentration measurements, significantly exceed reported DMS production rates for sub-surface waters. For example, in a compilation of 65 studies the maximum gross DMS production rates of 10–20 nmol L⁻¹ hr⁻¹ (Simó, 2004) were up to two orders of magnitude lower than the calculated PR_{SSM} based upon a 1000 µm SSM thickness. However, microorganisms in the SSM are exposed to extreme physicochemical conditions, including high irradiance (Zuev et al., 2001), whereas the DMS production rate estimates reported in Simó (2004) were from dark incubations that exclude the influence of light on DMS production. The conversion of intracellular DMSP to DMS is considered to be sensitive to both the quantity and spectra of light (Sunda et al., 2002; Archer et al., 2010),



and so exposure to high irradiance in the SSM will have a significant influence on DMS production. This is supported by the “DMS summer paradox” where higher DMSP and DMS levels have been observed in shallow mixed layers that are exposed to high light levels (Simó and Pedrós-Alió, 1999). Laboratory and field experiments have also demonstrated that DMS has a positive, dose-dependent response to solar radiation (Galí et al., 2013; Sunda et al., 2002; Vallina et al., 2007). In particular gross DMS production is stimulated by Ultra-Violet Radiation (UVR), which causes a reduction in algal cell integrity and enhanced release of DMSP, DMS and cleavage enzymes, and also up-regulation of intracellular DMSP cleavage (Galí et al., 2013). No relationship was observed between either $[DMS_{SSM}]$ or $[DMS_{6.0m}]$ with incident solar radiation in the current study, although this was confounded by differences in other factors such as phytoplankton biomass and community composition. The SSM was often sampled in the morning (0800–0930 h) which may suggest that the high DMS EFs in B1 may be a response to a night-day change in irradiance. Rapid changes in light can stimulate intracellular and dissolved DMSP production in coccolithophores (Darroch et al., 2015), with low-light cultures exposed to irradiance (including UVR) exhibiting an increase of 24–62 $\text{nmol L}^{-1} \text{h}^{-1}$ DMS (Archer et al., 2010). These production rates are still 1–2 orders of magnitude lower than many of the calculated PR_{SSM} for B1 (Table 1), but nevertheless confirm the potential for rapid DMS accumulation in response to increased light stress. Deck board incubations of SSM and SSS seawater from B2 and B3 stations showed that DMS production in the light was approximately double that in the dark (Cliff Law, pers. comm.), consistent with other reports (Galí et al., 2013). The highest net production rate of 3.7 $\text{nmol L}^{-1} \text{h}^{-1}$ in the light (Cliff Law, pers. comm.) was again substantially lower than the calculated PR_{SSM} in Table 1. Bacterial inhibition by high summertime UVR in the SSM (Zemmelink et al., 2006; Slezak et al., 2007) can decouple DMS production and consumption, with increased DMS observed in sub-surface waters (Vila-Costa et al., 2008). However, the absence of a significant difference in DMSP cycling between light and dark incubations of SSS during SOAP (Lizotte M. et al., submitted) suggests bacterial oxidation was not inhibited by light; although this was not measured in the SSM.

The different phytoplankton community composition of the three blooms may have influenced DMS enrichment in the SSM, particularly as all the blooms contained phytoplankton that are significant DMSP producers. B2 and B3 contained a higher proportion of coccolithophores but, despite evidence of their increased production of DMS and DMSP under high light stress (Archer et al., 2010), DMS levels were low in these two blooms. Conversely, B1 was dominated by dinoflagellates (>50 % of the phytoplankton biomass) and SSS $[DMS]$ levels and SSM enrichment were significantly higher. Dinoflagellates are significant DMSP producers, with intracellular DMSP content and DMSP lyase activity that generally exceeds that reported for coccolithophores (Caruana and Malin, 2014). Of four dominant dinoflagellate species in B1, *Gyrodinium* has been reported in association with high DMSP concentrations in the field (see Table 1, Caruana and Malin, 2014). Some dinoflagellate species migrate to the surface during the day, which influences the vertical distribution of associated DMSP and DMS. For example, a 10-fold increase in $[DMS]$ was recorded due to diel vertical migration of a dinoflagellate bloom in the St Lawrence River (Merzouk et al., 2004). Analysis of phytoplankton community composition at



the B1 stations showed only one dinoflagellate genus, *Ceratium*, which was more abundant at 1–2 cm relative to 2 m (data not shown), although this family does not generally exhibit high intracellular DMSP.

The EC data provide further evidence of a contribution of near-surface DMS production to air–sea flux, notably the close coincidence of significant EC- and SSM-derived residual [DMS] during B1 (Fig. 5c). The validity of this evidence is in part dependent upon generation of robust k values from the COARE model. Comparison with observational DMS datasets has confirmed that the COARE gas transfer model is a good predictor of k_{DMS} in most conditions, (Blomquist et al., 2006; Yang et al., 2011), including the SOAP voyage (Fig. 5b). A discrepancy with COARE has been reported under high winds ($> 11 \text{ m s}^{-1}$) in the North Atlantic, with lower measured k values attributed to the suppression of turbulence due to wind-wave interaction by Bell et al. (2013). In the current data analysis this suppression would result in a lower [DMS]_{inf}, in contrast to the elevated values of [DMS]_{inf} observed. In addition, the largest deviations between [DMS]_{inf} and [DMS]_{6.0m} during B1 occurred at mid-range wind speeds (6–8 m s^{-1} , Fig. 6a), where Bell et al. (2013) found good agreement with COARE. Consequently previous analysis does not indicate any significant bias in the COARE parameterization that could account for the high [DMS]_{inf} during B1.

Spatial decoupling of air and water side measurements inevitably introduces error into the estimate of residual [DMS]. For example, Bell et al. (2015) identify a spatial offset between measurements of DMS flux and seawater DMS of up to 2 km during SOAP. However this is unlikely to have generated the significant differences between [DMS]_{inf} and [DMS]_{6.0m} observed in B1, as these anomalies were observed when the ship was stationary or travelling slowly (< 2 knots), when wind speeds were $< 10 \text{ m s}^{-1}$ (see Fig. 5a). During these conditions, the flux footprint (Bell et al., 2015) would be much smaller. In addition, [DMS]_{inf} exceeded 20 nmol L^{-1} on a number of occasions during B1, whereas [DMS]_{6.0m} did not exceed 20 nmol L^{-1} throughout the entire voyage, suggesting that horizontal transport of DMS in the marine boundary layer from another bloom was not the source of the anomalously high [DMS]_{inf} during B1.

5 Summary

DMS fluxes are traditionally computed using [DMS] at depths below the air–sea interface; consequently significant near-surface DMS has important implications for flux estimates. Sub-surface [DMS] between 1 and 160 cm depth was relatively uniform at all stations on the Chatham Rise, in contrast to suggestions that DMS concentration should decrease near the air–sea interface as a result of surface sinks (Kieber et al., 1996). Although near-surface DMS gradients were generally absent, a significant exception was recorded in a dinoflagellate bloom during light to mid-range wind speeds (i.e. $< 10 \text{ m s}^{-1}$) and near-surface temperature stratification. On several occasions in this bloom, significant enrichment of DMS in the SSM coincided with measured DMS fluxes that exceeded predicted fluxes calculated using sub-surface [DMS] and the COARE algorithm. Although SSM enrichment of DMS (see Table 1) and anomalously high air–sea DMS fluxes have previously been reported (e.g. Marandino et al., 2008, 2007), this study’s results are the first to link these two phenomena.



There are some aspects of this dataset that are surprising, and require further investigation to establish the significance of the sea surface microlayer to air–sea DMS flux. For example, the study raises questions as to how significant DMS enrichment is maintained in the SSM without influencing the [DMS] in the underlying water. In addition, the elevated SSM [DMS] both measured and inferred from flux measurements in the dinoflagellate bloom B1, necessitates a substantial in-situ DMS production in the SSM. To maintain this enrichment, DMS production is required at a rate that significantly exceeds previous estimates for the open ocean (Simó, 2004). Nevertheless, the two independent approaches used in this study indicate that the SSM may influence DMS air–sea flux under certain biogeochemical and meteorological conditions, and so production at the air–sea interface may contribute to anomalously high DMS fluxes recorded in other regions of high productivity (Marandino et al., 2009, 2008).

6 Author contribution

C. Walker designed and conducted the experiments, developed and optimized the analytical methods and instrument, analysed the SSM and 1.6 m depth seawater samples for DMS, and interpreted the data. C. Walker also prepared the manuscript with contributions from C. Law, M. Harvey, M. Smith and T. Bell. C. Law helped with the experimental design, instrument optimisation, sample collection, data interpretation and drafting of the manuscript. C. Law also assisted with sampling logistics, and coordinated the overall measurement programme through his role as voyage leader. M. Harvey and J. McGregor assisted in the development of the analytical instrument, as did A. Marriner who also helped with the collection and analysis of seawater DMS samples. C. Law, M. Harvey and M. Smith provided invaluable mentoring and assisted with data interpretation and analysis. T. Bell and E. Saltzman supplied the air–sea DMS flux and Mini-CIMS seawater DMS data, and contributed to data interpretation.

7 Acknowledgements

The authors thank Captain Evan Solly and the crew of the R/V *Tangaroa* for their invaluable assistance with the field component of this study. We also thank Kim Currie (NIWA, Otago), Martine Lizotte (Laval University), Fiona Elliott (NIWA) and Karl Safi (NIWA, Hamilton) for their help in the collection and analysis of sea water samples and measurements, Christa Marandino, Warren DeBruyn and Cyril McCormick for their assistance with the supporting CIMS measurements. This research was supported by funding from NIWA's Climate and Atmosphere Research Programme 3 – role of the oceans (2015/16 SCI), and a Postdoctoral Fellowship (award number CO1X0911) for the New Zealand Ministry for Business, Innovation and Employment (MBIE). T. Bell and E. Saltzman were supported by the NSF Atmospheric Chemistry Program (grant nos. 08568, 0851472, 0851407 and 1143709).



8 References

- Agogu , H., Casamayor, E. O., Joux, F., Obernosterer, I., Dupuy, C., Lantoin , F., Catala, P., Weinbauer, M. G., Reinthaler, T., Herndl, G. J., and Lebaron, P.: Comparison of samplers for the biological characterization of the sea surface microlayer, *Limnology and Oceanography-Methods*, 2, 213-225, doi:10.4319/lom.2004.2.213, 2004.
- 5 Andreae, M. O., and Crutzen, P. J.: Atmospheric aerosols: Biogeochemical sources and role in atmospheric chemistry, *Science*, 276, 1052-1058, doi:10.1126/science.276.5315.1052, 1997.
- Archer, S. D., Ragni, M., Webster, R., Airs, R. L., and Geider, R. J.: Dimethyl sulfoniopropionate and dimethyl sulfide production in response to photoinhibition in *Emiliana huxleyi*, *Limnology and Oceanography*, 55, 1579-1589, doi:10.4319/lo.2010.55.4.1579, 2010.
- 10 Asher, W. E., Karle, L. M., Higgins, B. J., Farley, P. J., Monahan, E. C., and Leifer, I. S.: The influence of bubble plumes on air-seawater gas transfer velocities, *Journal of Geophysical Research: Oceans*, 101, 12027-12041, doi:10.1029/96JC00121, 1996.
- Ayers, G. P., and Gillett, R. W.: DMS and its oxidation products in the remote marine atmosphere: implications for climate and atmospheric chemistry, *Journal of Sea Research*, 43, 275-286, doi:10.1016/S1385-1101(00)00022-8, 2000.
- 15 Bandy, A. R., Thornton, D. C., Tu, F. H., Blomquist, B. W., Nadler, W., Mitchell, G. M., and Lenschow, D. H.: Determination of the vertical flux of dimethyl sulfide by eddy correlation and atmospheric pressure ionization mass spectrometry (APIMS), *Journal of Geophysical Research-Atmospheres*, 107, 4743, doi:10.1029/2002jd002472, 2002.
- Bell, T., De Bruyn, W., Marandino, C., Miller, S., Law, C., Smith, M., and Saltzman, E.: Dimethylsulfide gas transfer coefficients from algal blooms in the Southern Ocean, *Atmospheric Chemistry and Physics*, 15, 1783-1794, doi:10.5194/acp-15-1783-2015, 2015.
- 20 Bell, T. G., De Bruyn, W., Miller, S. D., Ward, B., Christensen, K. H., and Saltzman, E. S.: Air-sea dimethylsulfide (DMS) gas transfer in the North Atlantic: Evidence for limited interfacial gas exchange at high wind speed, *Atmospheric Chemistry and Physics*, 13, 11073-11087, doi:10.5194/acp-13-11073-2013, 2013.
- Blomquist, B. W., Fairall, C. W., Huebert, B. J., Kieber, D. J., and Westby, G. R.: DMS sea-air transfer velocity: Direct measurements by eddy covariance and parameterization based on the NOAA/COARE gas transfer model, *Geophysical Research Letters*, 33, L07601, doi:10.1029/2006GL025735, 2006.
- 25 Calleja, M. L., Duarte, C. M., Navarro, N., and Agust , S.: Control of air-sea CO₂ disequilibria in the subtropical NE Atlantic by planktonic metabolism under the ocean skin, *Geophysical Research Letters*, 32, L08606, doi:10.1029/2004GL022120, 2005.
- 30 Carlson, D. J.: Dissolved organic materials in surface microlayers: temporal and spatial variability and relation to sea state, *Limnology and Oceanography*, 28, 415-431, doi:10.4319/lo.1983.28.3.0415, 1983.
- Caruana, A. M. N., and Malin, G.: The variability in DMSP content and DMSP lyase activity in marine dinoflagellates, *Progress in Oceanography*, 120, 410-424, doi:10.1016/j.pocean.2013.10.014, 2014.



- Charlson, R. J., Lovelock, J. E., Andreae, M. O., and Warren, S. G.: Oceanic phytoplankton, atmospheric sulphur, cloud albedo and climate, *Nature*, 326, 655-661, doi:10.1038/326655a0, 1987.
- Cunliffe, M., Engel, A., Frka, S., Gašparović, B., Guitart, C., Murrell, J. C., Salter, M., Stolle, C., Upstill-Goddard, R., and Wurl, O.: Sea surface microlayers: A unified physicochemical and biological perspective of the air–ocean interface, *Progress in Oceanography*, 109, 104-116, doi:10.1016/j.pocean.2012.08.004, 2013.
- Cunliffe, M., and Wurl, O.: Guide to Best Practices to Study the Ocean's Surface, Occasional Publications of the Marine Biological Association of the United Kingdom, 118, 2014.
- Dacey, J. W. H., Wakeham, S. G., and Howes, B. L.: Henry law constants for dimethylsulfide in fresh-water and seawater, *Geophysical Research Letters*, 11, 991-994, doi:10.1029/GL011i010p00991, 1984.
- Darroch, L. J., Lavoie, M., Levasseur, M., Laurion, I., Sunda, W. G., Michaud, S., Scarratt, M., Gosselin, M., and Caron, G.: Effect of short-term light- and UV-stress on DMSP, DMS, and DMSP lyase activity in *Emiliania huxleyi*, *Aquatic Microbial Ecology*, 74, 173-185, doi:10.3354/ame01735, 2015.
- Edson, J. B., Hinton, A. A., Prada, K. E., Hare, J. E., and Fairall, C. W.: Direct covariance flux estimates from mobile platforms at sea, *Journal of Atmospheric and Oceanic Technology*, 15, 547-562, doi:10.1175/1520-0426(1998)015<0547:DCFEFM>2.0.CO;2, 1998.
- Fairall, C. W., Yang, M., Bariteau, L., Edson, J. B., Helmig, D., McGillis, W., Pezoa, S., Hare, J. E., Huebert, B., and Blomquist, B.: Implementation of the Coupled Ocean-Atmosphere Response Experiment flux algorithm with CO₂, dimethyl sulfide, and O₃, *Journal of Geophysical Research: Oceans*, 116, C00F09, doi:10.1029/2010JC006884, 2011.
- Galí, M., Simó, R., Pérez, G. L., Fuentes-Lema, A., Gasol, J. M., Royer, S. J., Ruiz-González, C., and Sarmiento, H.: Differential response of planktonic primary, bacterial, and dimethylsulfide production rates to static vs. dynamic light exposure in upper mixed-layer summer sea waters, *Biogeosciences*, 10, 7983-7998, doi:10.5194/bg-10-7983-2013, 2013.
- Garett, W. D.: Collection of slick-forming materials from the sea surface, *Limnology and Oceanography*, 10, 602-605, doi:10.4319/lo.1965.10.4.0602, 1965.
- Harvey, G. W.: Microlayer collection from the sea surface: A method and initial results, *Limnology and Oceanography*, 11, 608-613, doi:10.4319/lo.1966.11.4.0608, 1966.
- Harvey, G. W., and Burzell, L. A.: A simple microlayer method for small samples, *Limnology and Oceanography*, 17, 156-157, doi:10.4319/lo.1972.17.1.0156, 1972.
- Ho, D. T., Asher, W. E., Bliven, L. F., Schlosser, P., and Gordan, E. L.: On mechanisms of rain-induced air-water gas exchange, *Journal of Geophysical Research: Oceans*, 105, 24045-24057, doi:10.1029/1999JC000280, 2000.
- Ho, D. T., Law, C. S., Smith, M. J., Schlosser, P., Harvey, M., and Hill, P.: Measurements of air-sea gas exchange at high wind speeds in the Southern Ocean: implications for global parameterizations, *Geophysical Research Letters*, 33, L16611, doi:10.1029/2006GL026817, 2006.



- Ho, D. T., Wanninkhof, R., Schlosser, P., Ullman, D. S., Hebert, D., and Sullivan, K. F.: Toward a universal relationship between wind speed and gas exchange: Gas transfer velocities measured with $^3\text{He}/\text{SF}_6$ during the Southern Ocean Gas Exchange Experiment, *Journal of Geophysical Research-Oceans*, 116, C00F04, doi:10.1029/2010jc006854, 2011.
- Huebert, B. J., Blomquist, B. W., Hare, J. E., Fairall, C. W., Johnson, J. E., and Bates, T. S.: Measurement of the sea-air
5 DMS flux and transfer velocity using eddy correlation, *Geophysical Research Letters*, 31, L23113, doi:10.1029/2004GL021567, 2004.
- Kettle, A. J., and Andreae, M. O.: Flux of dimethylsulfide from the oceans: A comparison of updated data sets and flux models, *Journal of Geophysical Research: Atmospheres*, 105, 26793-26808, doi:10.1029/2000JD900252, 2000.
- Kieber, D. J., Jiao, J. F., Kiene, R. P., and Bates, T. S.: Impact of dimethylsulfide photochemistry on methyl sulfur cycling in
10 the equatorial Pacific Ocean, *Journal of Geophysical Research-Oceans*, 101, 3715-3722, doi:10.1029/95jc03624, 1996.
- Lana, A., Bell, T. G., Simo, R., Vallina, S. M., Ballabrera-Poy, J., Kettle, A. J., Dachs, J., Bopp, L., Saltzman, E. S., Stefels, J., Johnson, J. E., and Liss, P. S.: An updated climatology of surface dimethylsulfide concentrations and emission fluxes in the global ocean, *Global Biogeochemical Cycles*, 25, GB1004, doi:10.1029/2010gb003850, 2011.
- Law C. S. et al.: Southern Ocean Aerosol Production (SOAP): An Overview, *Atmospheric Physics and Chemistry*, ,
15 submitted.
- Liss, P. S., and Slater, P. G.: Flux of gases across the air-sea interface, *Nature*, 247, 181-184, doi:10.1038/247181a0, 1974.
- Liss, P. S.: Gas transfer: Experiments and geochemical implications, in: *Air-Sea Exchange of Gases and Particles*, edited by: Liss, P. S., and Slinn, W. G. N., NATO ASI Series, Springer Netherlands, 241-298, 1983.
- Liss, P. S., and Merlivat, L.: Air-sea gas exchange rates: Introduction and synthesis, in: *The Role of Air-Sea Exchange in
20 Geochemical Cycling*, edited by: Buat-Ménard, P., NATO ASI Series, Springer Netherlands, 113-127, 1986.
- Liss, P. S., and Duce, R. A.: *The Sea Surface and Global Change* [Online], in, edited by: Liss, P. S., and Duce, R. A., Cambridge University Press, Available from: Cambridge Books Online
<<http://dx.doi.org/10.1017/CBO9780511525025>>, Cambridge, 1997.
- Lizotte M. et al.: Converging facets of oceanic dimethylsulfoniopropionate (DMSP) and dimethylsulfide (DMS) bacterial
25 cycling across biological hotspots of the New Zealand Subtropical Front, *Ocean Science*, , submitted.
- Marandino, C. A., De Bruyn, W. J., Miller, S. D., and Saltzman, E. S.: Eddy correlation measurements of the air/sea flux of dimethylsulfide over the North Pacific Ocean, *Journal of Geophysical Research-Atmospheres*, 112, D03301, doi:10.1029/2006jd007293, 2007.
- Marandino, C. A., De Bruyn, W. J., Miller, S. D., and Saltzman, E. S.: DMS air/sea flux and gas transfer coefficients from
30 the North Atlantic summertime coccolithophore bloom, *Geophysical Research Letters*, 35, L23812, doi:10.1029/2008gl036370, 2008.
- Marandino, C. A., De Bruyn, W. J., Miller, S. D., and Saltzman, E. S.: Open ocean DMS air/sea fluxes over the eastern South Pacific Ocean, *Atmospheric Chemistry and Physics*, 9, 345-356, doi:10.5194/acp-9-345-2009, 2009.



- Matrai, P. A., Tranvik, L., Leck, C., and Knulst, J. C.: Are high Arctic surface microlayers a potential source of aerosol organic precursors?, *Marine Chemistry*, 108, 109-122, doi:10.1016/j.marchem.2007.11.001, 2008.
- McGillis, W. R., Dacey, J. W. H., Frew, N. M., Bock, E. J., and Nelson, R. K.: Water-air flux of dimethylsulfide, *Journal of Geophysical Research-Oceans*, 105, 1187-1193, doi:10.1029/1999jc900243, 2000.
- 5 Merzouk, A., Levasseur, M., Scarratt, M., Michaud, S., and Gosselin, M.: Influence of dinoflagellate diurnal vertical migrations on dimethylsulfoniopropionate and dimethylsulfide distribution and dynamics (St. Lawrence Estuary, Canada), *Canadian Journal of Fisheries and Aquatic Sciences*, 61, 712-720, doi:10.1139/f04-066, 2004.
- Momzikoff, A., Brinis, A., Dallot, S., Gondry, G., Saliot, A., and Lebaron, P.: Field study of the chemical characterization of the upper ocean surface using various samplers, *Limnology and Oceanography: Methods*, 2, 374-386, doi:10.4319/lom.2004.2.374, 2004.
- 10 Murphy, R. J., Pinkerton, M. H., Richardson, K. M., Bradford-Grieve, J. M., and Boyd, P. W.: Phytoplankton distributions around New Zealand derived from SeaWiFS remotely-sensed ocean colour data, *New Zealand Journal of Marine and Freshwater Research*, 35, 343-362, doi:10.1080/00288330.2001.9517005, 2001.
- Nguyen, B. C., Gaudrey, A., Bonsang, B., and Lambert, G.: Reevaluation of the role of dimethyl sulphide in the sulphur budget, *Nature*, 275, 637-639, doi:10.1038/275637a0, 1978.
- 15 Nightingale, P. D., Liss, P. S., and Schlosser, P.: Measurements of air-sea gas transfer during an open ocean algal bloom, *Geophysical Research Letters*, 27, 2117-2120, doi:10.1029/2000GL011541, 2000.
- Nightingale, P. D.: Air-sea gas exchange, in: *Surface Ocean-Lower Atmosphere Processes*, edited by: Le Quéré, C., and Saltzman, E. S., American Geophysical Union, 69-97, 2013.
- 20 Salter, M. E., Upstill-Goddard, R. C., Nightingale, P. D., Archer, S. D., Blomquist, B., Ho, D. T., Huebert, B., Schlosser, P., and Yang, M.: Impact of an artificial surfactant release on air-sea gas fluxes during Deep Ocean Gas Exchange Experiment II, *Journal of Geophysical Research: Oceans*, 116, C11016, doi:10.1029/2011JC007023, 2011.
- Saltzman, E. S., King, D. B., Holmen, K., and Leck, C.: Experimental determination of the diffusion coefficient of dimethylsulfide in water, *Journal of Geophysical Research: Oceans*, 98, 16481-16486, doi:10.1029/93JC01858, 1993.
- 25 Schmidt, R., and Schneider, B.: The effect of surface films on the air-sea gas exchange in the Baltic Sea, *Marine Chemistry*, 126, 56-62, doi:10.1016/j.marchem.2011.03.007, 2011.
- Simó, R., and Pedrós-Alió, C.: Short-term variability in the open ocean cycle of dimethylsulfide, *Global Biogeochemical Cycles*, 13, 1173-1181, doi:10.1029/1999GB900081, 1999.
- Simó, R.: Production of atmospheric sulfur by oceanic plankton: Biogeochemical, ecological and evolutionary links, *Trends Ecol. Evol.*, 16, 287-294, doi:10.1016/s0169-5347(01)02152-8, 2001.
- 30 Simó, R.: From cells to globe: approaching the dynamics of DMS(P) in the ocean at multiple scales, *Canadian Journal of Fisheries and Aquatic Sciences*, 61, 673-684, doi:10.1139/f04-030, 2004.



- Slezak, D., Kiene, R. P., Toole, D. A., Simó, R., and Kieber, D. J.: Effects of solar radiation on the fate of dissolved DMSP and conversion to DMS in seawater, *Aquatic Sciences*, 69, 377-393, doi:10.1007/s00027-007-0896-z, 2007.
- Sunda, W., Kieber, D. J., Kiene, R. P., and Huntsman, S.: An antioxidant function for DMSP and DMS in marine algae, *Nature*, 418, 317-320, doi:10.1038/nature00851, 2002.
- 5 Swan, H. B., Armishaw, P., Iavetz, R., Alamgir, M., Davies, S. R., Bell, T. G., and Jones, G. B.: An interlaboratory comparison for the quantification of aqueous dimethylsulphide, *Limnology and Oceanography: Methods*, 12, 784-794, 2014.
- Sweeney, C., Gloor, E., Jacobson, A. R., Key, R. M., McKinley, G., Sarmiento, J. L., and Wanninkhof, R.: Constraining global air-sea gas exchange for CO₂ with recent bomb ¹⁴C measurements, *Global Biogeochemical Cycles*, 21, GB2015, doi:10.1029/2006GB002784, 2007.
- 10 Swinbank, W. C.: The measurement of vertical transfer of heat and water vapor by eddies in the lower atmosphere, *Journal of Meteorology*, 8, 135-145, doi:10.1175/1520-0469(1951)008<0135:TMOVTO>2.0.CO;2, 1951.
- Toole, D. A., and Siegel, D. A.: Light-driven cycling of dimethylsulfide (DMS) in the Sargasso Sea: closing the loop, *Geophysical Research Letters*, 31, L09308, doi:10.1029/2004GL019581, 2004.
- 15 Turner, S. M., and Liss, P. S.: Measurements of various sulphur gases in a coastal marine environment, *Journal of Atmospheric Chemistry*, 2, 223-232, doi:10.1007/BF00051074, 1985.
- Turner, S. M., Malin, G., Liss, P. S., Harbour, D. S., and Holligan, P. M.: The seasonal variation of dimethyl sulfide and dimethylsulfoniopropionate concentrations in nearshore waters¹, *Limnology and Oceanography*, 33, 364-375, doi:10.4319/lo.1988.33.3.0364, 1988.
- 20 Vallina, S. M., Simo, R., Gasso, S., De Boyer-Montegut, C., del Rio, E., Jurado, E., and Dachs, J.: Analysis of a potential "solar radiation dose-dimethylsulfide-cloud condensation nuclei" link from globally mapped seasonal correlations, *Global Biogeochemical Cycles*, 21, doi:10.1029/2006gb002787, 2007.
- Vila-Costa, M., Kiene, R. P., and Simó, R.: Seasonal variability of the dynamics of dimethylated sulfur compounds in a coastal northwest Mediterranean site, *Limnology and Oceanography*, 53, 198-211, doi:10.4319/lo.2008.53.1.0198, 25 2008.
- Walker, C. F., Harvey, M. J., Bury, S. J., and Chang, F. H.: Biological and physical controls on dissolved dimethylsulfide over the north-eastern continental shelf of New Zealand, *Journal of Sea Research*, 43, 253-264, doi:10.1016/S1385-1101(00)00017-4, 2000.
- Wanninkhof, R.: Relationship between Wind-Speed and Gas-Exchange over the Ocean, *Journal of Geophysical Research-Oceans*, 97, 7373-7382, doi:10.4319/lom.2014.12.351, 1992.
- 30 Wanninkhof, R., Sullivan, K. F., and Top, Z.: Air-sea gas transfer in the Southern Ocean, *Journal of Geophysical Research: Oceans*, 109, C08S19, doi:10.1029/2003JC001767, 2004.



- Wolfe, G. V., Strom, S. L., Holmes, J. L., Radzio, T., and Olson, M. B.: Dimethylsulfoniopropionate cleavage by marine phytoplankton in response to mechanical, chemical, or dark stress, *Journal of Phycology*, 38, 948-960, doi:10.1046/j.1529-8817.2002.t01-1-01100.x, 2002.
- Woolf, D. K.: Parametrization of gas transfer velocities and sea-state-dependent wave breaking, *Tellus B*, 57, 87-94, doi:10.1111/j.1600-0889.2005.00139.x, 2005.
- Wurl, O., Wurl, E., Miller, L., Johnson, K., and Vagle, S.: Formation and global distribution of sea-surface microlayers, *Biogeosciences*, 8, 121-135, doi:10.5194/bg-8-121-2011, 2011.
- Yang, G.-P., Jing, W.-W., Li, L., Kang, Z.-Q., and Song, G.-S.: Distribution of dimethylsulphide and dimethylsulfoniopropionate in the surface microlayer and sub-surface water of the Yellow Sea, China during spring, *Journal of Marine Systems*, 62, 22-34, doi:10.1016/j.jmarsys.2006.04.003, 2006.
- Yang, G.-P., Jing, W.-W., Kang, Z.-Q., Zhang, H.-H., and Song, G.-S.: Spatial variations of dimethylsulphide and dimethylsulfoniopropionate in the surface microlayer and in the sub-surface waters of the South China Sea during springtime, *Marine Environmental Research*, 65, 85-97, doi:10.1016/j.marenvres.2007.09.002, 2008.
- Yang, G.-P., Levasseur, M., Michaud, S., Merzouk, A., Lizotte, M., and Scarratt, M.: Distribution of dimethylsulphide and dimethylsulfoniopropionate and its relation with phytoneuston in the surface microlayer of the western North Atlantic during summer, *Biogeochemistry*, 94, 243-254, doi:10.1007/s10533-009-9323-y, 2009.
- Yang, G. P.: Dimethylsulfide enrichment in the surface microlayer of the South China Sea, *Marine Chemistry*, 66, 215-224, doi:10.1016/S0304-4203(99)00042-0, 1999.
- Yang, G. P., Watanabe, S., and Tsunogai, S.: Distribution and cycling of dimethylsulfide in surface microlayer and subsurface seawater, *Marine Chemistry*, 76, 137-153, doi:10.1016/s0304-4203(01)00054-8, 2001.
- Yang, G. P., Levasseur, M., Michaud, S., and Scarratt, M.: Biogeochemistry of dimethylsulphide (DMS) and dimethylsulfoniopropionate (DMSP) in the surface microlayer and sub-surface water of the western North Atlantic during spring, *Marine Chemistry*, 96, 315-329, doi:10.1016/j.marchem.2005.03.003, 2005a.
- Yang, G. P., and Tsunogai, S.: Biogeochemistry of dimethylsulfide (DMS) and dimethylsulfoniopropionate (DMSP) in the surface microlayer of the western North Pacific. , *Deep Sea Research Part I: Oceanographic Research Papers*. , 52, 553-567, doi:10.1016/j.dsr.2004.11.013, 2005.
- Yang, G. P., Tsunogai, S., and Watanabe, S.: Biogenic sulfur distribution and cycling in the surface microlayer and sub-surface water of Funka Bay and its adjacent area, *Continental Shelf Research*, 25, 557-570, doi:10.1016/j.csr.2004.11.001, 2005b.
- Yang, M., Blomquist, B. W., Fairall, C. W., Archer, S. D., and Huebert, B. J.: Air-sea exchange of dimethylsulfide in the Southern Ocean: Measurements from SO GasEx compared to temperate and tropical regions, *Journal of Geophysical Research: Oceans*, 116, C00F05, doi:10.1029/2010JC006526, 2011.



- Yoch, D. C.: Dimethylsulfoniopropionate: Its sources, role in the marine food web, and biological degradation to dimethylsulfide, *Applied and Environmental Microbiology*, 68, 5804-5815, doi:10.1128/aem.68.12.5804-5815.2002, 2002.
- Zemmelink, H. J., Dacey, J. W. H., and Hintsa, E. J.: Direct measurements of biogenic dimethylsulphide fluxes from the oceans: a synthesis, *Canadian Journal of Fisheries and Aquatic Sciences*, 61, 836-844, doi:10.1139/f04-047, 2004.
- 5 Zemmelink, H. J., Houghton, L., Sievert, S. M., Frew, N. M., and Dacey, J. W. H.: Gradients in dimethylsulfide, dimethylsulfoniopropionate, dimethylsulfoxide, and bacteria near the sea surface, *Marine Ecology-Progress Series*, 295, 33-42, doi:10.3354/meps295033, 2005.
- Zemmelink, H. J., Houghton, L., Frew, N. M., and Dacey, J. W. H.: Dimethylsulphide and major sulfur compounds in a stratified coastal salt pond, *Limnology and Oceanography*, 51, 271-279, doi:10.4319/lo.2006.51.1.0271, 2006.
- 10 Zhang, H.-H., Yang, G.-P., and Zhu, T.: Distribution and cycling of dimethylsulphide (DMS) and dimethylsulfoniopropionate (DMSP) in the sea-surface microlayer of the Yellow Sea, China, in spring, *Continental Shelf Research*, 28, 2417-2427, 2008.
- Zhang, H. H., Yang, G. P., Liu, C. Y., and Li, C. X.: Seasonal variations of dimethylsulphide (DMS) and dimethylsulfoniopropionate (DMSP) in the sea-surface microlayer and sub-surface water of Jiaozhou Bay and its adjacent area, *Acta Oceanologica Sinica*, 28, 73-86, 2009.
- 15 Zhang, Z., Liu, L., Liu, C., and Cai, W.: Studies on the sea surface microlayer: II. The layer of sudden change of physical and chemical properties, *Journal of Colloid and Interface Science*, 264, 148-159, doi:10.1016/S0021-9797(03)00390-4, 2003.
- 20 Zuev, B., Chudinova, V., Kovalenko, V., and Yagov, V.: The conditions of formation of the chemical composition of the sea surface microlayer and techniques for studying organic matter in it, *Geochemistry International c/c of Geokhimiia*, 39, 702-710, 2001.



9 Tables

DOY	Date/time	Lat	Lon	[DMS] _{1.6m}	[DMS] _{SSM}	EF	PR _{SSM_100µm}	PR _{SSM_1000µm}
UTC	NZDT	°	°	nM	nM		nmol L ⁻¹ h ⁻¹	nmol L ⁻¹ h ⁻¹
	dd/mm/yy							
	HH:MM							
B1								
45.8	15/02/12 08:05	44.62S	174.77E	4.9±0.8	26.1±0.0	5.3	1153±522	115±52
46.8	16/02/12 08:06	44.59S	174.68E	13.6±0.6	25.9±8.2	1.9	-486±270	-49±27
47.1	16/02/12 15:51	44.59S	174.69E	13.8±n/a	19.9±n/a	1.4	n/a	n/a
47.8	17/02/12 08:02	44.59S	174.69E	9.2±2.0	41.5±9.7	4.5	5529±655	553±66
48.8	18/02/12 08:04	44.59S	174.69E	5.9±0.4	4.1±0.2	0.7	2468±454	247±45
Mean				9.5±0.1	23.5±9.3	2.8	2166±1623	217±162
B2								
52.8	22/02/12 08:27	43.72S	179.86W	6.9±0.2	8.7±1.1	1.3	-1445±348	-145±35
55.0	23/02/12 13:03	43.59S	179.75W	7.1±1.8	7.0±0.0	1.0	-153±52	-15.3±5
Mean				7.0±1.8	7.9±1.0	1.2	-799±333	-80±33
B3								
58.1	27/02/12 14:39	44.11S	175.14E	8.7±0.0	5.0±0.2	0.6	614±162	61±16
59.8	29/02/12 08:03	44.60S	174.87E	6.6±0.9	3.8±0.4	0.6	867±129	87±13
64.8	05/03/12 09:04	44.18S	174.33E	10.5±0.1	10.2±1.1	1.0	n/a	n/a
65.1	05/03/12 14:12	44.18S	174.33E	6.3±0.0	7.1±0.8	1.1	n/a	n/a
Mean				8.0±1.1	6.5±1.3	0.8	740±224	74±22

- 5 **Table 1:** SSM station variables: DMS concentration in the SSM ([DMS]_{SSM}), collected using the plate method, and in seawater at 1.6 m
 depth ([DMS]_{1.6m}); DMS enrichment factor (EF); and DMS production rate (PR_{SSM}) for a 100 µm and 1000 µm thick microlayer. Day of
 year (DOY) is where 1 is January 1st at 00:00 h. [DMS] errors are 1 standard deviation from the mean of duplicate samples. EF is the
 ratio of microlayer and 1.6 m concentrations, with an EF > 1 indicating enrichment and <1 depletion. Inferred SSM production rates were
 10 calculated using the EC flux, assuming a SSM thickness of 100 µm and 1000 µm. Production rates are averages for the period three hours
 before and five hours after microlayer sampling.



10 Figures

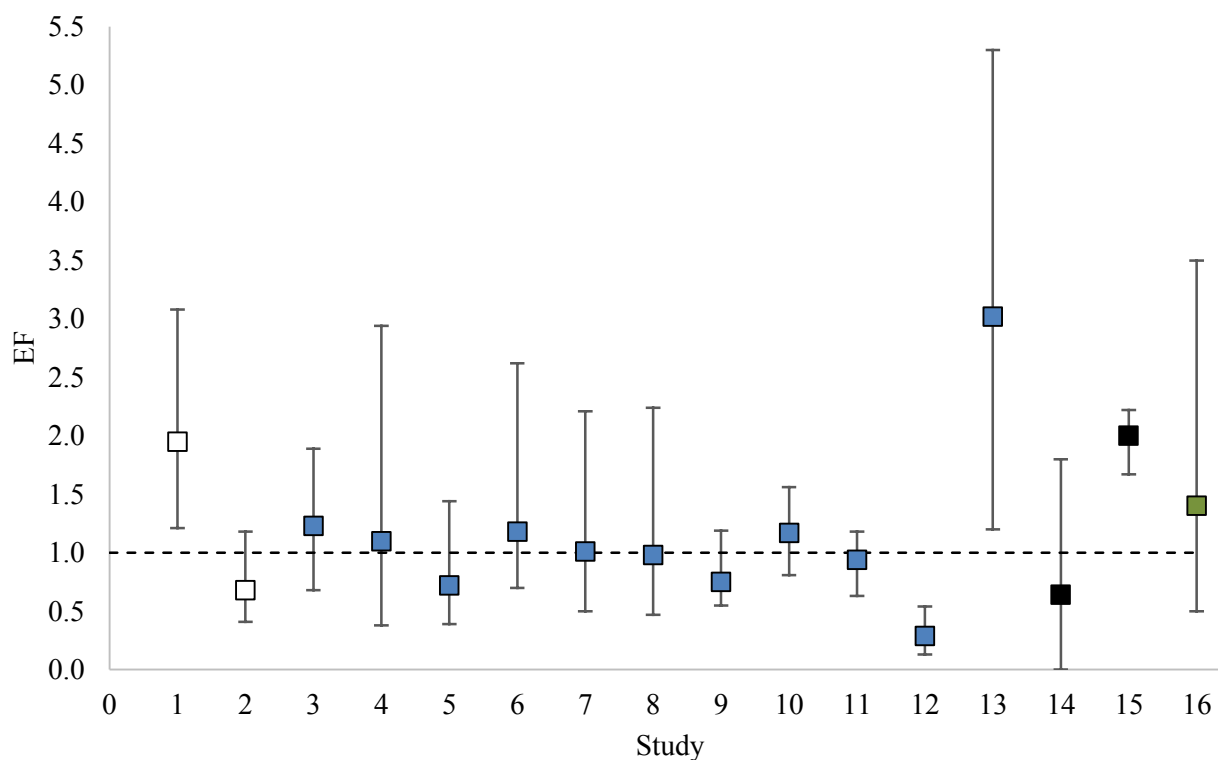


Figure 1: Mean enrichment factors (EF) for DMS in the SSM reported in previous studies. Upper and lower bars indicate the highest and lowest value reported in each study. An EF of 1.0, shown by the horizontal dashed line, indicates no difference between [DMSSSM] and [DMSSSS], with EF > 1 denoting enrichment in the SSM relative to SSS, and values < 1 a deficit relative to SSS. The sampling method is indicated by the symbol colour: plate (white), mesh (blue), drum (black) and cryogenic (grey). References: 1 (Yang, 1999); 2 & 3 (Yang et al., 2001); 4 (Yang and Tsunogai, 2005); 5 (Yang et al., 2005a); 6 (Yang et al., 2005b); 7 (Yang et al., 2006); 8 (Zhang et al., 2008); 9 (Yang et al., 2008); 10 & 11 (Zhang et al., 2009); 12 (Yang et al., 2009); 13 (Matrai et al., 2008); 14 (Zemmelink et al., 2006); 15 (Turner and Liss, 1985); 16 (Nguyen et al., 1978).

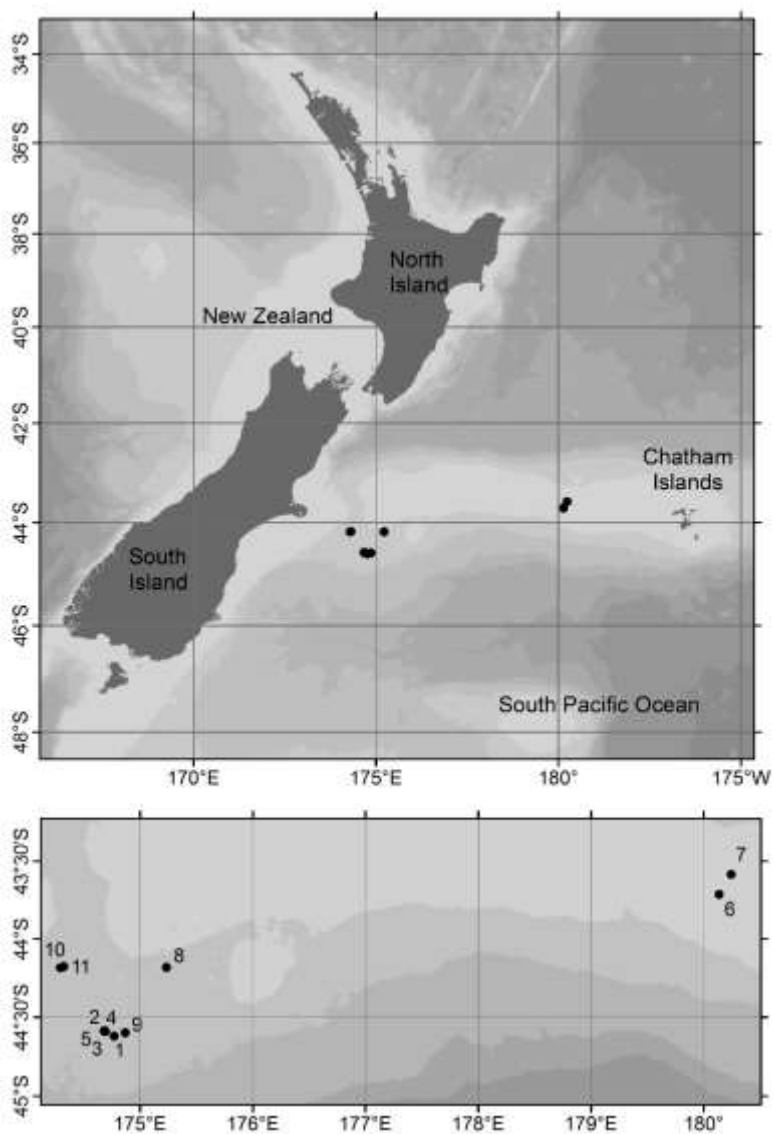


Figure 2: A map of New Zealand waters showing the location of the eleven SSM sampling stations (black dots), with station numbers shown in the expanded Chatham Rise region in the lower panel. Blooms B1, B2, and B3 encompass stations 1 – 5, 6 – 7, and 8 – 11, respectively.

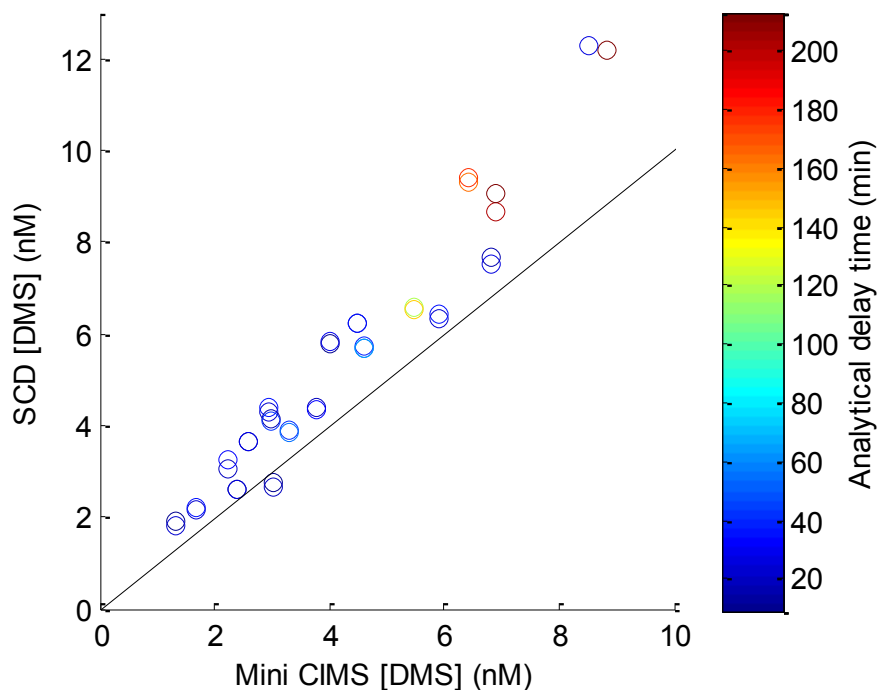


Figure 3: Comparison between [DMS] measured using the Mini-CIMS and SCD methods. Colour bar indicates the time elapsed between sample collection and analysis on the SCD. Mini-CIMS analysis was near real-time so data are averaged over a 1 hour period surrounding the SCD sample collection. The black solid line is 1:1.

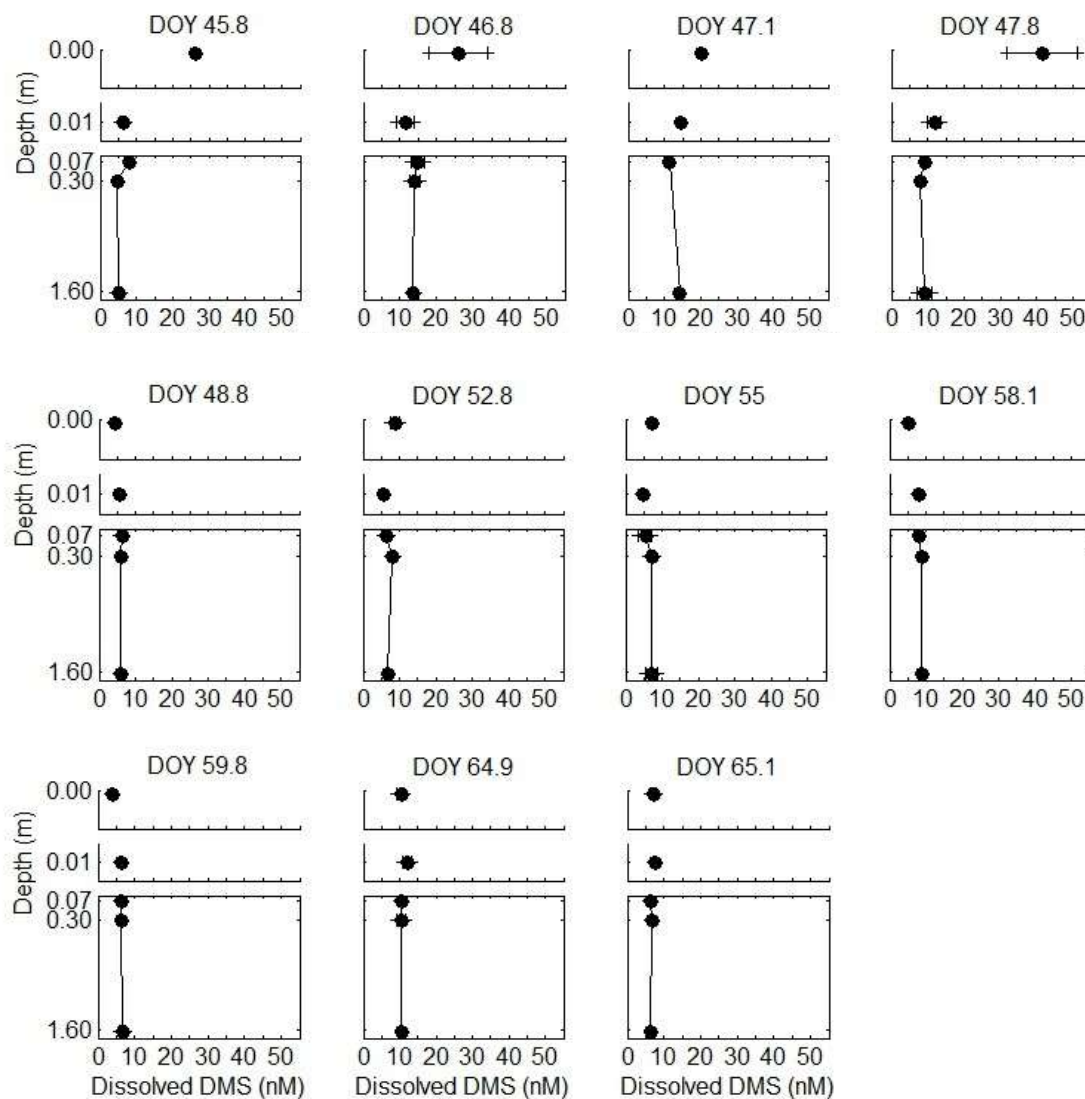


Figure 4: Near-surface concentration gradients of [DMS] in the SSM and in the upper 1.6 m. Measurements presented are the mean replicate samples, and error bars represent one standard deviation.

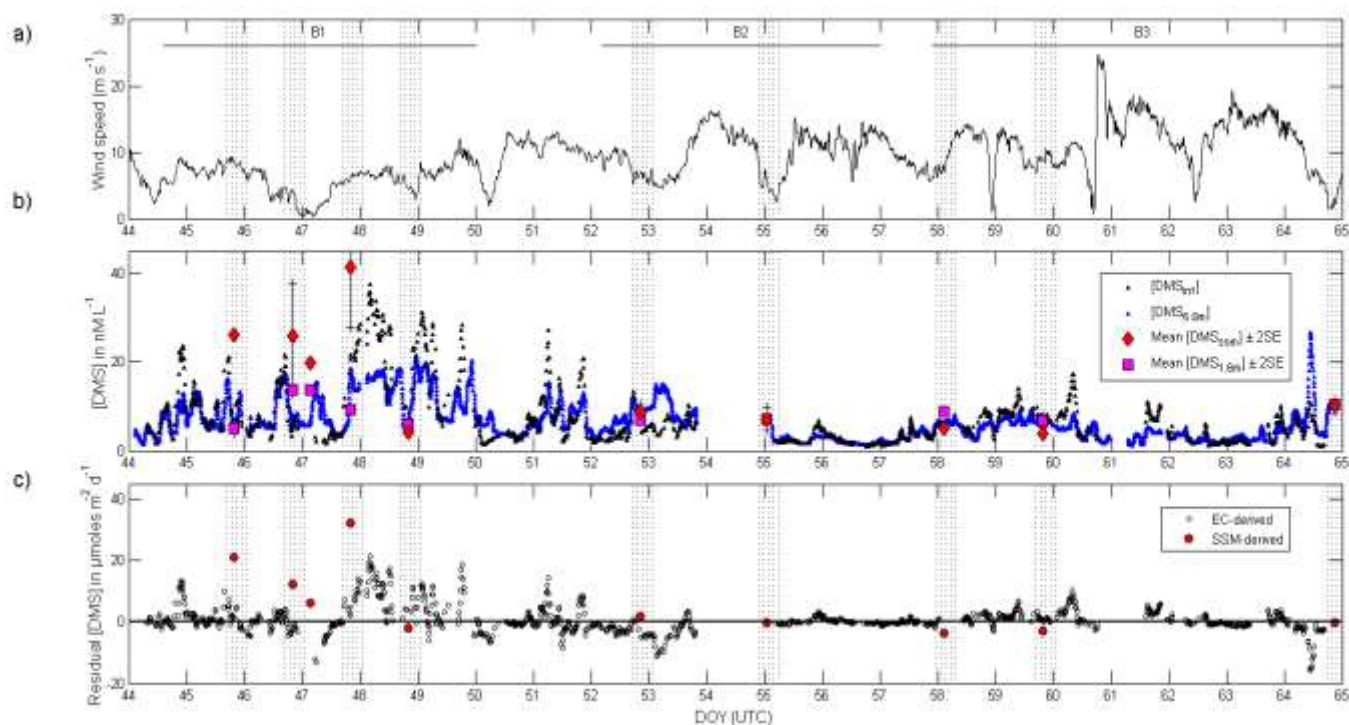


Figure 5: a) Wind speed normalized to 10 m. b) Flux-inferred concentrations of seawater DMS ([DMS_{inf}] black triangles), overlain with the mean for [DMS_{ssm}] (red diamonds), [DMS_{1.6m}] (pink squares), and [DMS_{6.0m}] (blue triangles). [DMS_{inf}] was calculated from continuous EC flux measurements and COARE k values based on local conditions. [DMS_{inf}] and [DMS_{6.0m}] datasets were smoothed using a moving average algorithm with a span of 1 hour. Error bars indicate 2 x standard error of the mean of replicate samples. Shaded areas indicate the period from 3 hours prior, to and 5 hours after SSM sampling. Periods encompassing intense sampling within algal blooms (B1, B2 and B3) are indicated by the horizontal lines at the top of the graph. SSM measurements for DOY 47.1 and 65.1 coincide with a gap in EC air-sea flux data. On DOY 48.8, changes in [DMS_{6.0m}] during station occupation indicate the SSM sample is unlikely to be representative of the SSM for the entire station. c) SSM-derived residual [DMS] (red circles) compared with EC-derived residual [DMS] (black circles).

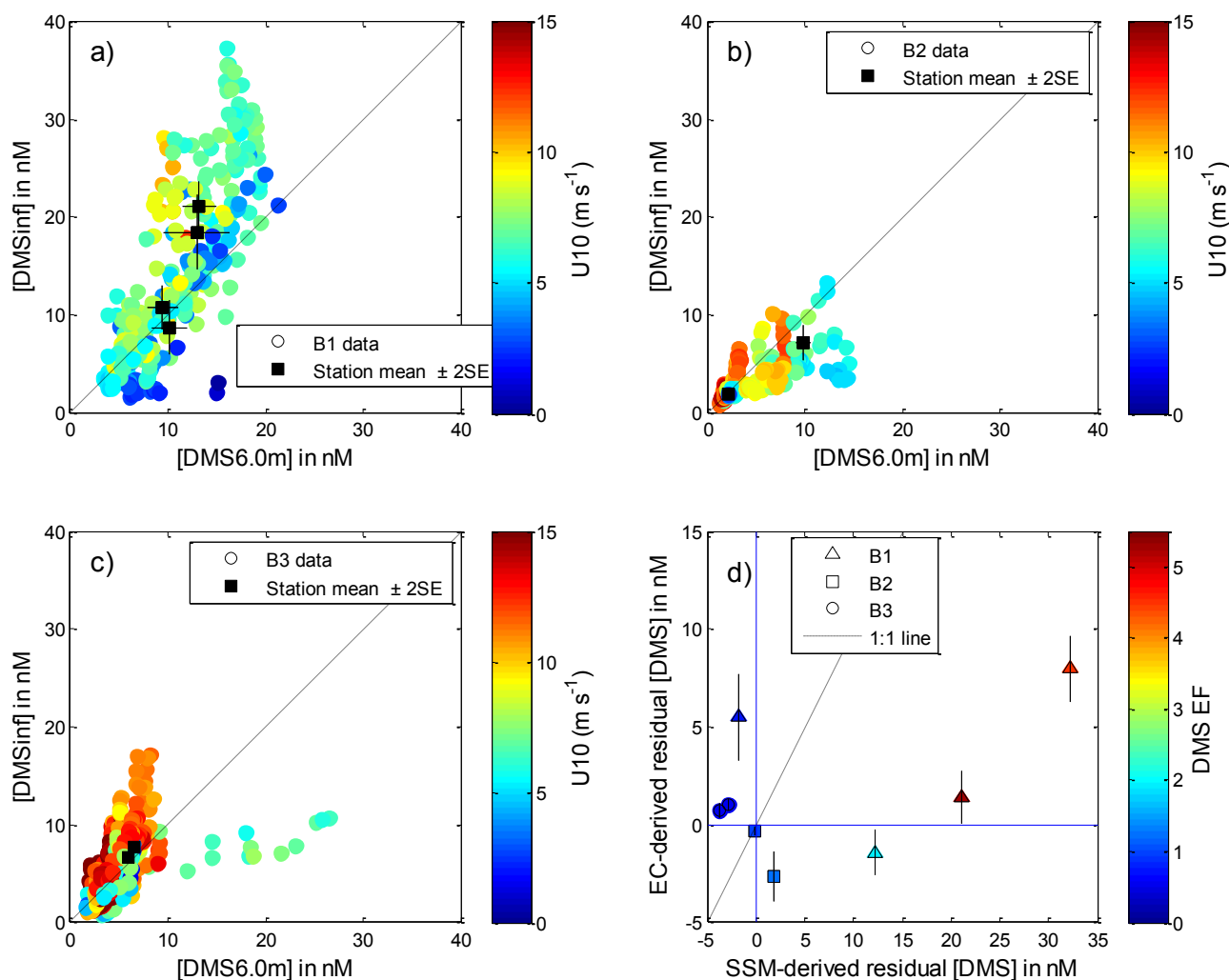


Figure 6 (a – c): Comparison between smoothed [DMS_{inf}] and [DMS_{6.0m}] (10 min intervals) during each bloom period. The dashed line indicates the 1:1 relationship. The black squares indicate the mean during the period from 3 hours prior to 5 hours post-sampling the SSM, with error bars indicating 2 x the Standard Error. The symbol colour indicates wind speed (U_{10}), as shown in the colour bar. d) Relationship between SSM-derived residual [DMS] and EC-derived residual [DMS] for each SSM station. Data is not available for stations sampled on DOY 47.1, 64.8 and 65.1. Solid vertical and horizontal lines indicate zero residual [DMS], and the dashed line the 1:1 relationship. Symbol colour indicates enrichment factor (EF). The periods used to calculate station means are denoted by shading in Fig. 4.

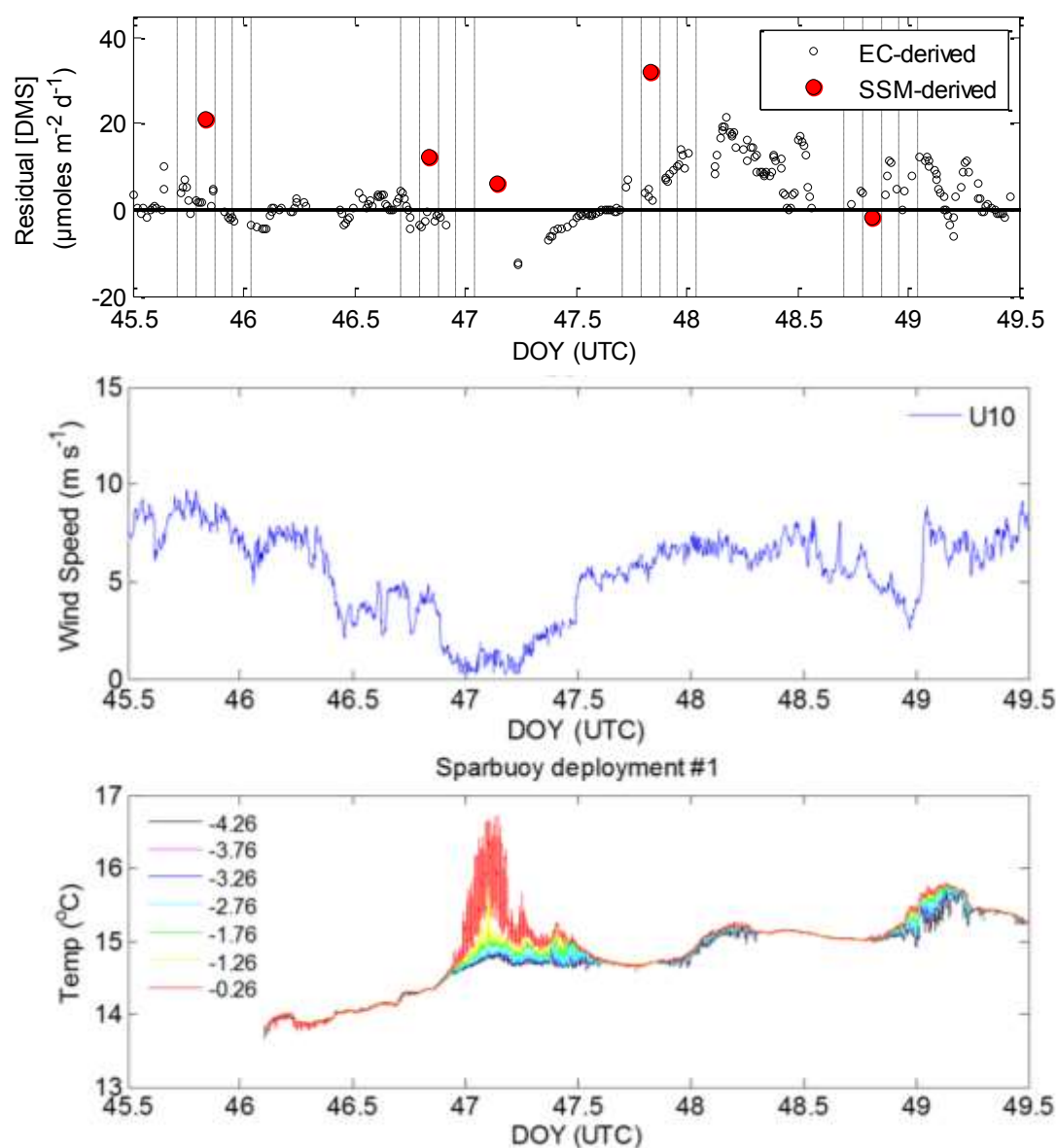


Figure 7: The period between DOY 45.5 and 49.5 in Bloom 1 showing: SSM-derived residual [DMS] (red circles) and EC-derived [DMS] (black circles) in the top plot. SSM measurements for DOY 47.1 coincided with a gap in EC air-sea flux data. Vertical dashed lines indicate the period from 3 hours before to 5 hours after sampling. Wind speed normalized to 10 m (middle plot). Near surface temperatures (bottom plot; legend shows depth in metres).